TECHNISCHE MECHANIK, 36, 3, (2016), 180 – 189
submitted: October 29, 2015

About the Vibration Modes of Square Plate-like Structures

F. Duvigneau, S. Koch, R. Orszulik, E. Woschke, U. Gabbert

In the experimental vibration analysis of an oil pan, two eigenmodes are observed that did not appear to be those of a standard rectangular plate vibration. As a result, a numerical, analytical and experimental investigation is launched to discover where these modes are originating from. In this paper, the finite element method is applied to determine the vibration behavior numerically, and experimental results are obtained with the help of a laser doppler vibrometer in order to determine the origin of these two eigenmodes.

1 Introduction

The motivation of this paper is due to the results found from an experimental modal analysis of the oil pan of a two cylinder diesel engine. In general, such a thin oil pan bottom shows a vibration behavior similar to that of a plate, but in Fig. 1(a) and (b) two vibration modes are exhibited which do not match with the typical modes of a rectangular plate.

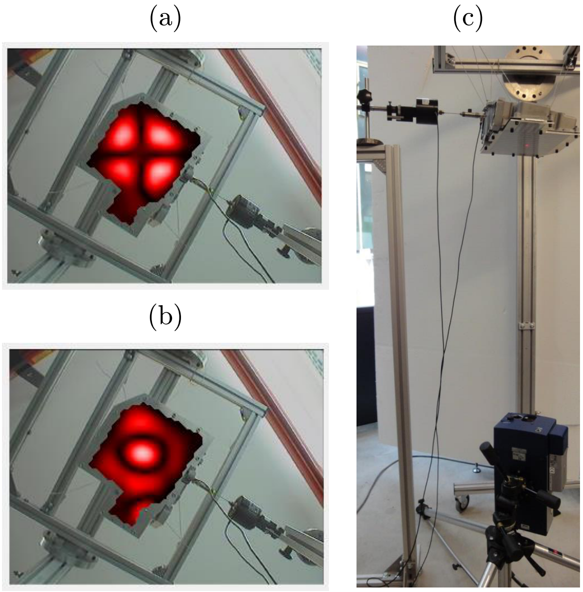

Figure 1: Measured vibration modes of an oil pan bottom at (a) 599 Hz, (b) 630 Hz, with (c) showing the experimental setup used for the measurements.

The vibration response of plates is well understood and it is easy to check the plausibility of the results from numerical models by using the analytical solution of the problem. Consequently, we searched for the explanation of the unexpected vibration modes seen in Fig. 1 by investigating the known solutions for rectangular plates in the literature. However, both the numerical and the analytical solutions for rectangular plates never calculate modes with a shape like that seen in Fig. 1 for any configuration.
However, it is also possible to approximate the oil pan bottom of Fig. 1 as a perfectly square plate. The numerical solution for this configuration shows the unexpected vibration modes of Fig. 1, but no longer the typical vibration modes (see Fig. 2, second row), which are also observable in the experimental results of the oil pan bottom (see

Fig. 2, first row). Thus, the aim of this paper is to find out why the experimental results show a mixture of these mode types and also to find the influential parameters that define which of the respective rectangular and square vibration modes will appear.

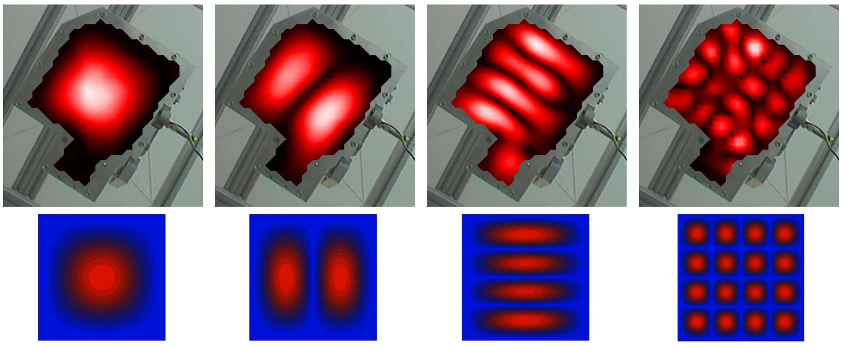

Figure 2: Typical vibration modes of a plate-like structure from experimental (top) and numerical (bottom) results

In the literature of the second half of the 20th century many publications exist about the vibration of square plates. Most of these are based on the analytical solution as the mathematical description of the problem has not significantly changed over the years. Johns and Nataraja (1972), Vijayakumar and Ramaiah (1978), Banerjee (1982), Chaudhuri (1984), Tabarrok et al. (1987), Downs (1989), and Batra et al. (2004) have all investigated square plates. Unfortunately, all of these publications do not show the mode shapes of the investigated plates, only the eigenfrequencies. Yang and Sethna (1991, 1992) calculate the vibration behavior of plates which differ only slightly from ideal square plates. Further, Irie et al. (1983), and Laura and Bacha de Natalini (1983) research plates with round corners and Genesan and Nagaraja Rac (1985), and Sakiyama et al. (2003) investigate several cut-outs of thin square plates, however none of them show any mode shapes of the vibrating plates.
In Shimon and Hurmuzlu (2007), the vibration behavior of a fully clamped square plate that takes into account some temperature variations is studied both numerically and experimentally in the context of vibration control. In contrast to the findings in the paper at hand, it is curious that Shimon and Hurmuzlu (2007) only show the typical modes of a rectangular plate instead of a square one. Shojaee et al. (2012) also calculate the vibrations of square plates under different boundary conditions, which also only show the typical modes of a rectangular plate.
On the contrary, Jhung and Jeong (2015) show the mode shapes of a square plate. In their study the focus is on a perforated square plate with fixed edges in the context of nuclear energy. However, purely numerical studies are performed and thus only square modes are observed and not a mixture of the mode shapes of a square and a rectangular plate. Saha et al. (2004), Saha et al. (2005) analyze the influence of different boundary conditions on the vibration behavior of square plates numerically and take into account geometric nonlinearities caused by the consideration of large deformations. However, they also do not show this mixture of mode shapes for the case of a fully clamped square plate. In addition, Wilson et al. (2000) give experimental results for partially clamped square plates and also observe in some cases atypical mode shapes. Olson and Hazell (1979) study the vibrations of a square, built-in plate with axissymmetric, parabolically varying thickness both theoretically and experimentally. They state that the vibration modes are seen to exhibit an interesting blend of radial and square symmetries, but do not discuss the phenomenom addressed in this paper. Additionally, problems in the agreement between the experimental and numerical results in the lower frequency domain are observed.

2 Numerical Models

In this section the numerical modelling is presented. All simulations in this paper are executed with the help of the finite element method (Hughes, 1987). To calculate the vibrations of the structure, the linear system of equations can be written as

$$\mathbf{M}_u \ddot{\mathbf{u}}(\mathbf{x}, t) + \mathbf{C}_u \dot{\mathbf{u}}(\mathbf{x}, t) + \mathbf{K}_u \mathbf{u}(\mathbf{x}, t) = \mathbf{f}_u(t) \tag{1}$$

where $\mathbf{M}_u$ denotes the mass matrix, $\mathbf{C}_u$ the damping matrix and $\mathbf{K}_u$ the stiffness matrix of the system. Furthermore, in Eq. (1) $\ddot{\mathbf{u}}(\mathbf{x}, t)$ denotes the acceleration, $\dot{\mathbf{u}}(\mathbf{x}, t)$ the velocity, $\mathbf{u}(\mathbf{x}, t)$ the displacement and $\mathbf{f}_u(t)$ the external time dependent loads of the system. The time integration of Eq. (1) requires very small time steps, hence the vibration analysis is carried out exclusively in the frequency domain to minimize the computational costs. Transformation into the frequency domain by a harmonic time approach via $\mathbf{u}(\mathbf{x}, t) = \tilde{\mathbf{u}}(\mathbf{x}) e^{\mathrm{i}\Omega t}$ and

$\mathbf{f}_u\,(t) = \tilde{\mathbf{f}_u} e^{\mathrm{i}\Omega t}$ results in

$$\left(-\Omega^2 \mathbf{M}_u + \mathrm{i}\Omega \mathbf{C}_u + \mathbf{K}_u\right) \tilde{\mathbf{u}}\,(\mathbf{x}) = \tilde{\mathbf{f}_u} \tag{2}$$

where $\tilde{\mathbf{u}}$ denotes the complex amplitude of the displacements, $\tilde{\mathbf{f}}_u$ the vector of the frequency dependent external loads, i the imaginary unit and Ω the angular frequency of the excitation of the system. The damping in Eq. (2) is neglected to calculate the real eigenfrequencies f_i and eigenmodes $\mathbf{\Psi}_i\,(\mathbf{x})$. The classical eigenvalue problem in matrix notation is written as

$$\left(-\left(2\pi f_i\right)^2 \mathbf{M}_u + \mathbf{K}_u\right) \mathbf{\Psi}_i\,(\mathbf{x}) = 0 \quad . \tag{3}$$

The question to be answered is why the numerical results for the vibration analysis of a square plate show such modes as in Fig. 1. Hence, it is investigated whether these modes are induced by any numerical effects. For this reason, different meshes are analyzed, from ideal structured to irregular meshes, which are shown in Fig. 3. The boundary conditions are defined as in the classical analytical solution of rectangular plates for comparability. With the help of smooth rounded corners (see Fig. 3, left) it is also checked whether the corners influence the modes.

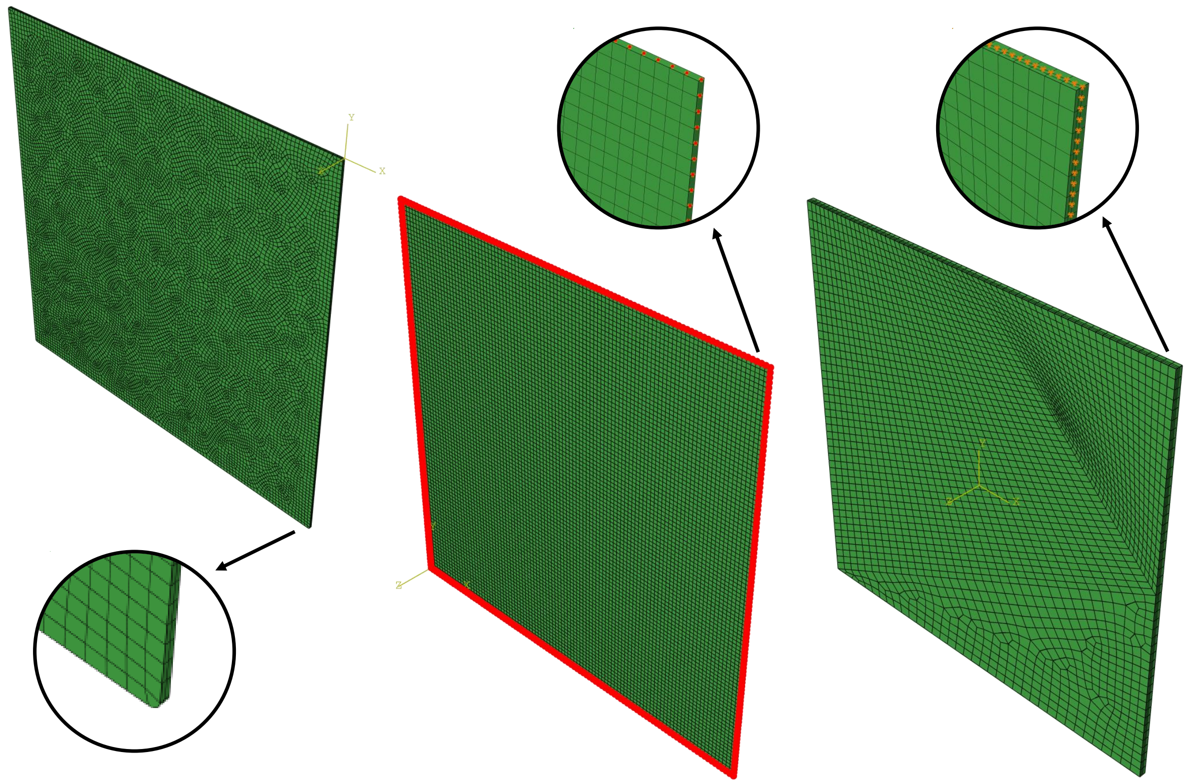

Figure 3: Different numerical models of a square plate

It quickly becomes clear that different discretizations and boundary conditions can change the numerical results slightly, but the special mode shapes are preserved. These special mode shapes can lead to the conclusion that the modes of a circular plate are appearing, since every square can be circumscribed by a circle, while also inscribing one. To prove this hypothesis the numerical model in Fig. 4 is generated and its mode shapes calculated.

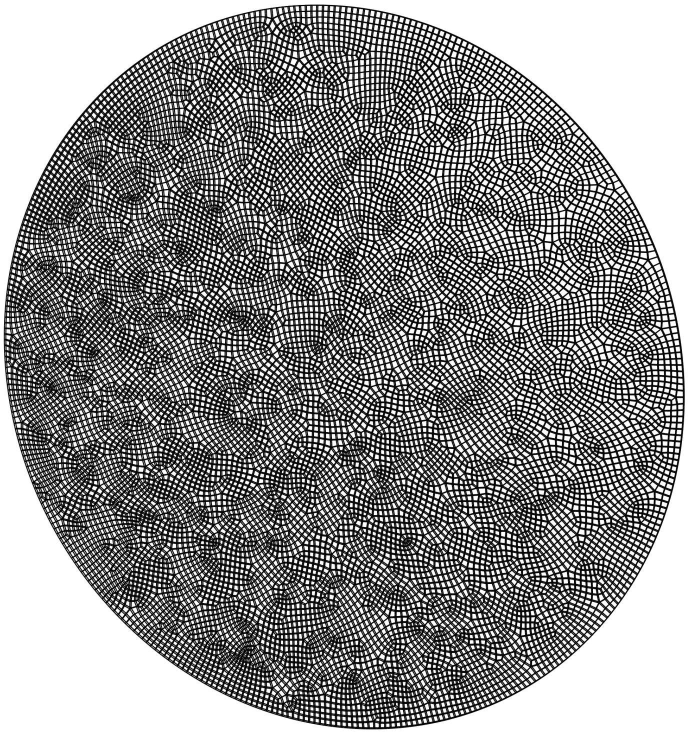

Figure 4: Numerical model of the circular plate

In Fig. 5, the comparison between the modes of the circular and the square plate is shown. The modes are similar, as they have similar dimensions and they are symmetric structures, but the eigenfrequencies of the respective modes show a very poor correspondence to each other. The influence of the radius was also investigated and it can be stated that the differences in the eigenfrequencies cannot be overcome by varying the radius of the circle.

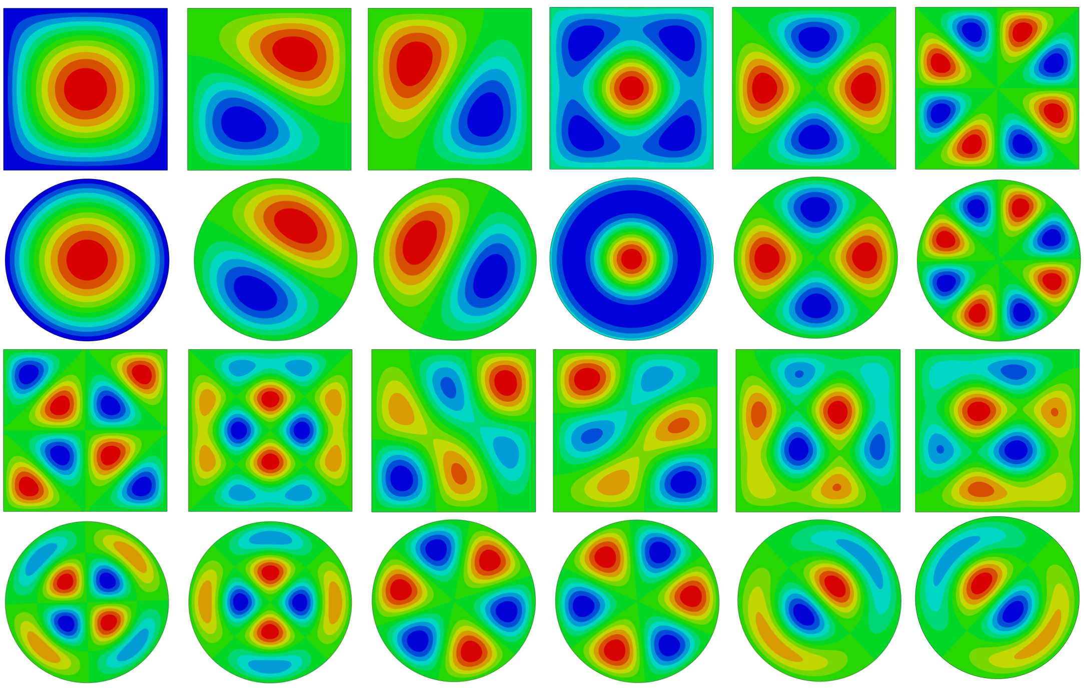

Figure 5: Comparison of the mode shapes of a square and a circular plate

3 Analytical Solution

The analytical solution for the modal behavior of rectangular plates is given in Eq. (4) and Eq. (6). Eq. (4) shows the calculation of the eigenfrequency f_{mn} of a rectangular plate with length l_1 in the x_1-direction and length l_2 in the x_2-direction.

$$f_{mn} = \frac{\pi}{2}\sqrt{\frac{K}{\rho t}}\left(\left(\frac{m}{l_1}\right)^2 + \left(\frac{n}{l_2}\right)^2\right); \quad m = 1, ..., \infty; \quad n = 1, ..., \infty \tag{4}$$

Alongside the density ρ and the thickness t, the plate stiffness K is an important parameter which can be calculated as

$$K = \frac{Et^3}{12(1-\nu^2)} \quad . \tag{5}$$

In Eq. (5) ν is Poisson's ratio and E is the modulus of elasticity. The calculation of the eigenmodes of a rectangular plate is given as

$$\Psi_{mn}(x_1, x_2) = \sin\left(\frac{m\pi}{l_1}x_1\right)\sin\left(\frac{n\pi}{l_2}x_2\right) \quad . \tag{6}$$

In the case that length l_1 and l_2 are identical, it is easy to see from Eq. (4) that there always exist two combinations of m and n which result in the same eigenfrequency f_{mn} as long as $m \neq n$. However, the corresponding eigenmodes are not identical, hence, a superposition of each mode must appear (Giurgiutiu, 2014). The orthogonality condition is naturally still fulfilled as the positive and negative superpositions of orthogonal eigenmodes are also still orthogonal to all other eigenmodes.

In Fig. 6 two examples are shown in detail. On the left hand side the superposition of the $\mathbf{\Psi}_{13}$ and $\mathbf{\Psi}_{31}$ modes is demonstrated and on the right hand side the superposition of the $\mathbf{\Psi}_{35}$ and $\mathbf{\Psi}_{53}$ modes. The middle row contains the pair of analytical plate modes with the same eigenfrequency, while the first row contains the positive and the third row the negative superposition of the analytical modes. Additionally, in the first and third row the corresponding numerical solution is given. From the comparison of the mode shapes and their respective eigenfrequencies, it is obvious that the reason for the special mode shapes is due to the positive and negative superposition of the two eigenmodes with the same eigenfrequency. Fig. 6 and 7 show that the numerical and analytical results match quite well in both the eigenmodes and the eigenfrequencies.

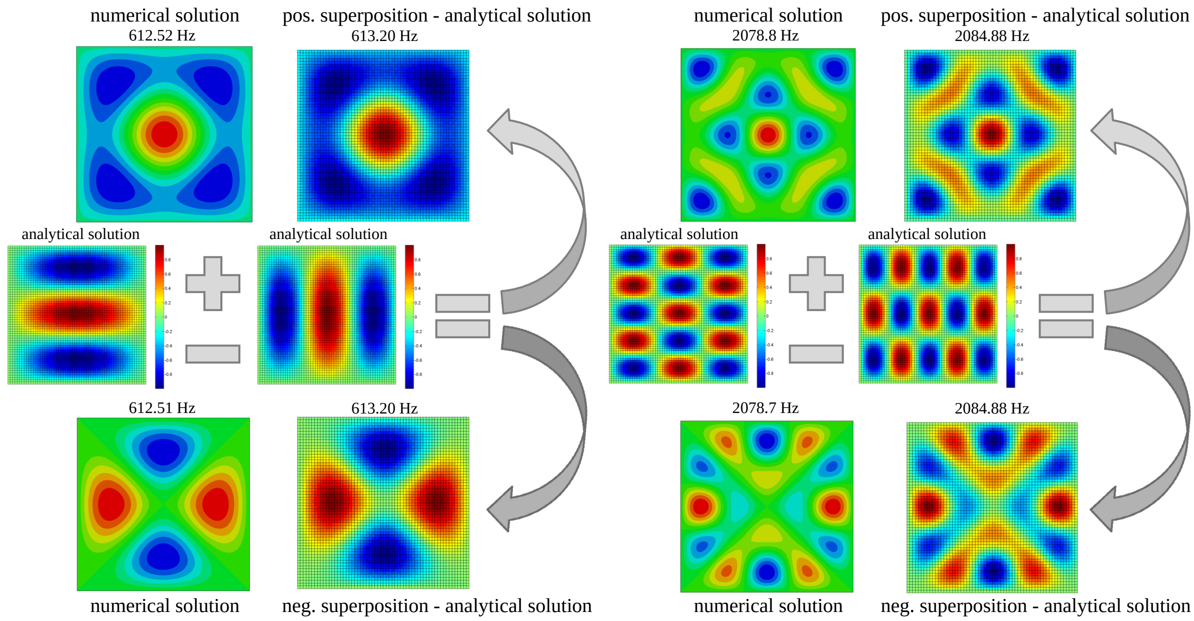

Figure 6: Positive (first row) and negative (third row) superpositions of the analytically calculated eigenmodes of a square plate in comparison to the numerical results

The left hand side of Fig. 6 also shows the two modes which are observed in the measurement of the oil pan bottom in Fig. 1. The question is why both superpositions (the positive and the negative one) are observable in the experiment and appear at different frequencies, since the calculated eigenfrequencies are very close to each other or even identical in the case of the analytical solution. Furthermore, it is also not clear why only some of the mode pairs are appearing in their superposed forms in the experimental results. In the numerical and analytical results of a modal analysis of a square plate only the superpositions appear (see Fig. 7).

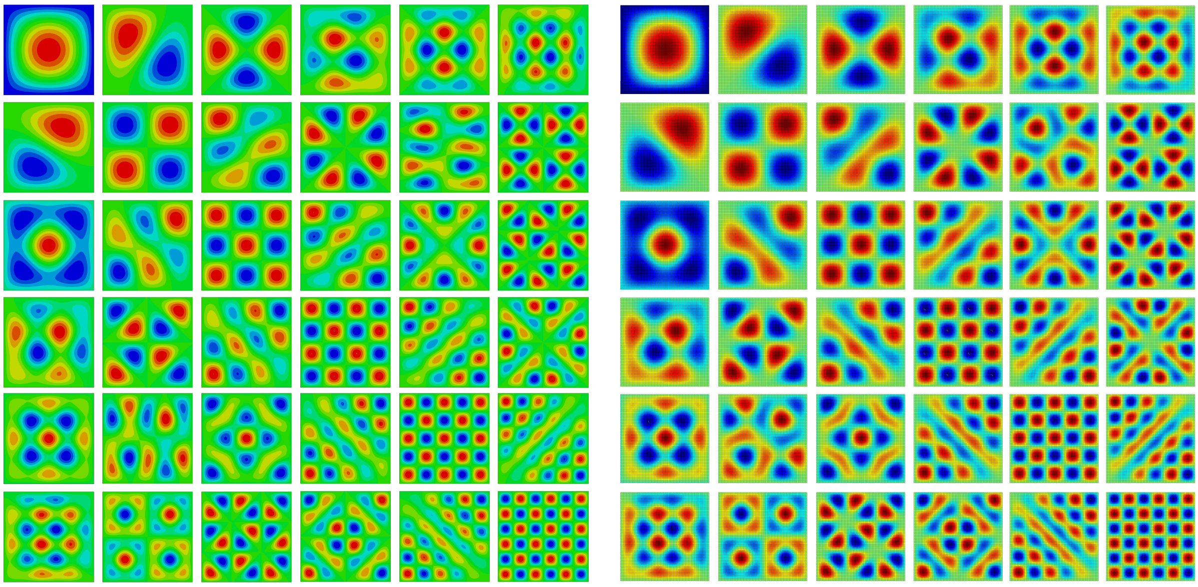

Figure 7: Comparison of numerically (left) and analytically (right) calculated eigenmodes of a square plate

4 Experimental Results

In this section the phenomenon is investigated experimentally to clarify the questions why only some of the superpositions are observed in the measurements of Fig. 1, which modes are affected, and what are the parameters of influence.

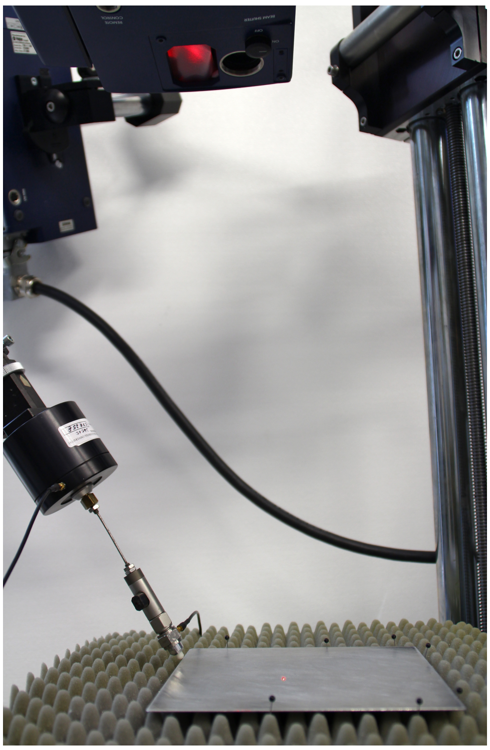

Figure 8: Experimental setup for the modal analysis of the thin square plate under free-free boundary conditions

Fig. 8 shows the experimental setup for the determination of the mode shapes of a thin square plate via a scanning laser vibrometer from Polytec (PSV-400). The plate is made out of $1mm$ thick aluminum and is square with edge lengths of $100mm$. The laser head has to be vertically positioned with respect to the plate to minimize the measurement error, since a one-dimensional scanning vibrometer is used. The mounting of the square plate is realized with free-free boundary conditions via soft foam which can be seen in Fig. 8. Additionally, pins are used to avoid horizontal rigid body movements of the plate. Moreover, an electro-dynamic shaker (Mini Shaker Type 4810, Brüel & Kjær) with an impact hammer head (Force Transducer Type 2800, Brüel & Kjær) is used to generate the excitation (see Fig. 8). For the force sensor in the hammer head the Charge Amplifier Type 2635 (Brüel & Kjær) is used and for the excitation signal to the electro-dynamic shaker the Power Amplifier Type 2706 (Brüel & Kjær) is used. The combination of the electro-dynamic shaker and the impact hammer head provides the opportunity to apply an automated, controlled and programmable excitation without changing the boundary conditions. Consequently, it is still possible to realize free-free boundary conditions for the experimental setup in Fig. 8. This is important to guarantee that the influence of the experimental setup on the measured vibration behavior of the thin plate is minimal.
To make the measurements, the shaker is programmed with an impulse excitation, which shows the shape of a half sinus with a frequency of $51.2Hz$. This impulse has a length of $5ms$ and was repeated every $1.6s$. Thus, this defined excitation signal is able to excite frequencies up to $2000Hz$. The shaker is mounted on a separate frame to avoid unintended secondary vibration paths from the shaker to the structure. The following specifications are used for the laser-vibrometer measurements: a high order low-pass filter with a cut-off frequency of $2000Hz$, a sampling frequency of $5120Hz$, three averages and a rectangular windowing technique.

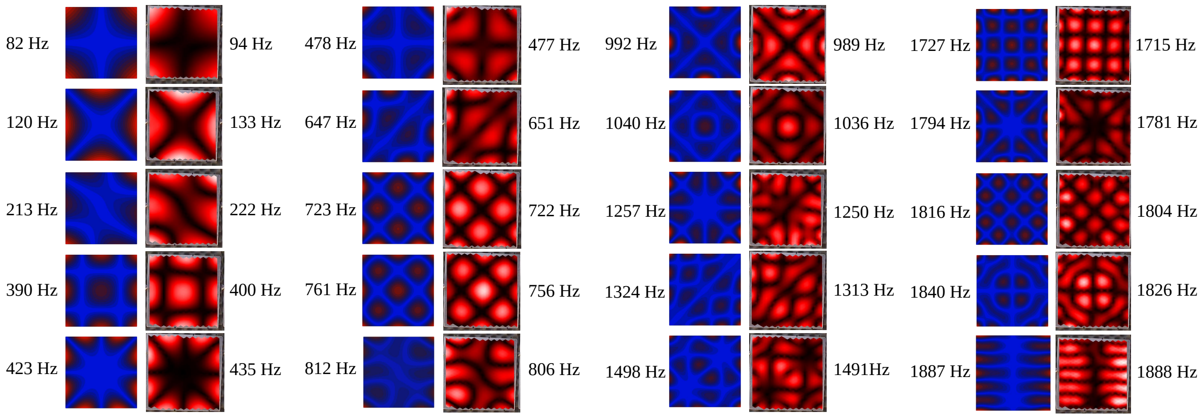

Figure 9: Comparison of the numerical (left columns) and experimental (right columns) modal analyses of the thin square plate under free-free boundary conditions

The results of the numerical and experimental modal analysis of the thin square plate under free-free boundary conditions are compared explicitly for 20 different eigenmodes in Fig. 9. Due to the experimental modal analysis it is important to take into account the position of the excitation, as only excited eigenmodes are observable. Consequently, superpositions of two eigenmodes with the same eigenfrequency can only appear if both are excited with the same intensity. If one eigenmode shows much higher vibration amplitudes than the other, only the dominant eigenmode is observable. These facts are confirmed by several measurements with different excitation points.
In general, Fig. 9 shows a lot of superpositions and that the numerical and experimental results agree very well in terms of both the mode shapes and the frequencies. Hence, it is assumed that the boundary conditions play an important role due to the open question of why only some of the superpositions are observed in the measurement in Fig. 1. For this reason, the aluminum plate is studied under clamped boundary conditions. The experimental setup used is shown in Fig. 10 and is designed in such a way that the part of the plate that is not fixed has the same dimensions as the plate under free-free boundary conditions in Fig. 8. It should be noted that both experimental setups are identical except for the boundary conditions of the plate.
In Fig. 11 the comparison of the numerical and experimental modal analysis of the thin square plate under clamped boundary conditions can be seen. It is obvious that only one superposition (see the experimental result at 699 Hz) is still appearing in the experimental results of the clamped plate and that this mode is the same one that is observed in the oil pan bottom of Fig. 1.

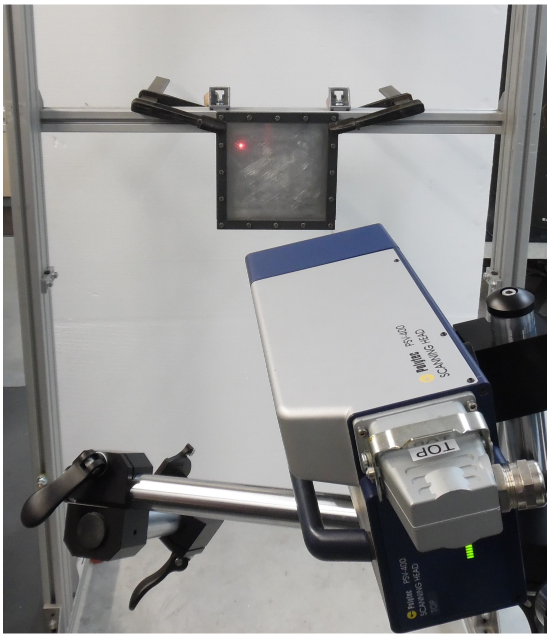

Figure 10: Experimental setup for the modal analysis of the thin square plate under clamped boundary conditions

The experiment was repeated a few times with a new clamped plate assembly to secure that the free part of the plate was as close to an ideal square as possible, but the results are the same. Hence, it would seem that only some special eigenmode-superpositions are robust enough to still appear under clamped boundary conditions.

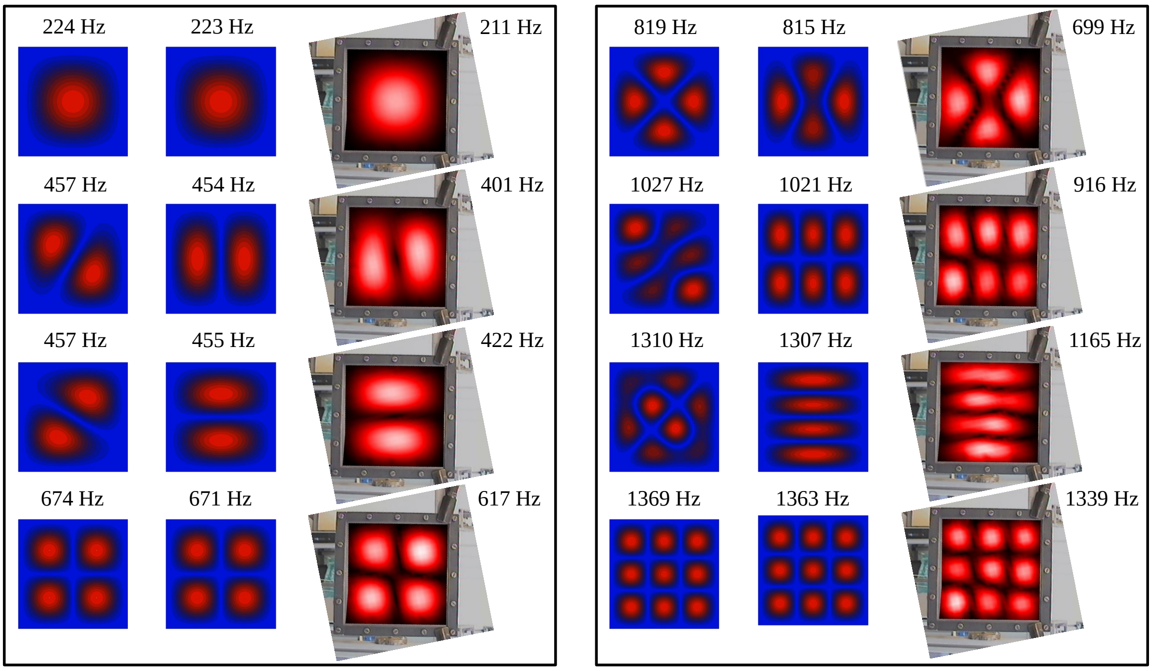

Figure 11: Comparison of the numerical and experimental modal analysis of the thin square plate under clamped boundary conditions. Left columns: numerical results of the perfect square plate, middle columns: numerical results of the square plate with geometric imperfections, right columns: experimental results of the clamped square plate.

In Fig. 11 each measured eigenmode is compared with two numerically calculated modes on its left hand side. The left column of each of the two numerical eigenmodes is calculated based on an ideal square model with an edge length of $100mm$. Consequently, it shows the superposed modes as were seen in Section 2 and 3, which are not observable in the corresponding experimental results in Fig. 11. The numerical results in the middle columns are obtained by increasing the edge length by 0.5% as an imperfection in order to consider the difference from the ideal symmetric state, as most likely appears in reality. It is obvious that this approach works very well and the calculated eigenmodes are very similar to the measured ones. As usual, the calculated eigenfrequencies are higher than the measured ones, as the clamping of the experimental setup is much stiffer than the thin plate, but still elastic. Moreover, it is extremely important to note that the same "robust" superposition of modes is detected as in the numerical and experimental results (see $815Hz$ and $699Hz$ in the first row on the right hand side of Fig. 11).

5 Conclusion

In this paper the anomaly of the vibration modes of square plate-like structures is investigated numerically, analytically and experimentally. It can be stated that in the case of square plates, there appear positive and negative superpositions of eigenmode-pairs which have the same eigenfrequency. These superpositions are analytically, numerically and experimentally observable under free-free boundary conditions. Under clamped boundary conditions only a few robust superpositions still appear in the experimental results. To consider this fact in simulations, a model should be used that possesses some small imperfections or asymmetries. In this paper, the slight increase of one edge length has been shown to be a very efficient way to induce such an imperfection and to predict the robust modes.

Acknowledgments

The presented work is part of the joint project COMO "Competence in Mobility", which is financially supported by the European Union as well as the German State of Saxony-Anhalt. This support is gratefully acknowledged. We also would like to thank Steffen Liefold for his help.

References

Banerjee, B.: Large amplitude vibrations of a clamped orthotropic square plate carrying a concentrated mass. *Journal of Sound and Vibration*, 82, (1982), 329 – 333.

Batra, R. C.; Qian, L. F.; Chen, L. M.: Natural frequencies of thick square plates made of orthotropic, trigonal, monoclinic, hexagonal and triclinic materials. *Journal of Sound and Vibration*, 270, (2004), 1074 – 1086.

Chaudhuri, S. K.: Large amplitude free vibrations of a square plate of variable thickness. *Journal of Sound and Vibration*, 92, (1984), 143 – 147.

Downs, B.: Anticlastic curvature correction of a square plate finite element applied to the transverse vibration of flat plates. *Journal of Sound and Vibration*, 131, (1989), 249 – 258.

Genesan, N.; Nagaraja Rac, S.: Influence of location of cut-outs on natural frequencies of thin square plates. *Journal of Sound and Vibration*, 101, (1985), 598 – 600.

Giurgiutiu, V.: *Structural Health Monitoring with Piezoelectric Wafer Active Sensors (Second Edition) - Chapter 4*. Academic Press (2014).

Hughes, T. J. R.: *The Finite Element Method: Linear Static and Dynamic Finite Element Analysis*. Prentice-Hall, New Jersey (1987).

Irie, T.; Yamada, G.; Sonoda, M.: Natural frequencies of square membrane and square plate with rounded corners. *Journal of Sound and Vibration*, 86, (1983), 442 – 448.

Jhung, M. J.; Jeong, K. H.: Free vibration analysis of perforated plate with square penetration pattern using equivalent material properties. *Nuclear Engineering and Technology*, 47, (2015), 500 – 511.

Johns, D. J.; Nataraja, R.: Vibration of a square plate symmetrically supported at four points. *Journal of Sound and Vibration*, 25, (1972), 75 – 82.

Laura, P. A. A.; Bacha de Natalini, L.: Comments on ñatural frequencies of square membrane and square plate with rounded corners̈. *Journal of Sound and Vibration*, 91, (1983), 595 – 596.

Olson, M. D.; Hazell, C. R.: Vibrations of a square plate with parabolically varying thickness. *Journal of Sound and Vibration*, 62, (1979), 399 – 410.

Saha, K. N.; Misra, D.; Ghosal, S.; Pohit, G.: Nonlinear free vibration analysis of square plates with various boundary conditions. *Journal of Sound and Vibration*, 287, (2005), 1031 – 1044.

Saha, K. N.; Misra, D.; Pohit, G.; Ghosal, S.: Large amplitude free vibration study of square plates under different boundary conditions through a static analysis. *Journal of Vibration Control*, 10, (2004), 1009 – 1028.

Sakiyama, T.; Huang, M.; Matsuda, H.; Morita, C.: Free vibration of orthotropic square plates with a square hole. *Journal of Sound and Vibration*, 259, (2003), 63 – 80.

Shimon, P.; Hurmuzlu, Y.: A theoretical and experimental study of advanced control methods to suppress vibrations in a small square plate subject to temperature variations. *Journal of Sound and Vibration*, 302, (2007), 409 – 424.

Shojaee, S.; Izadpanah, E.; Valizadeh, N.; Kiendl, J.: Free vibration analysis of thin plates by using a nurbs-based isogeometric approach. *Finite Elements in Analysis and Design*, 61, (2012), 23 – 34.

Tabarrok, B.; Fenton, R. G.; Elsaie, A. M.: Lateral vibration of square plates subject to in-plane loadings. *Journal of Sound and Vibration*, 112, (1987), 295 – 303.

Vijayakumar, K.; Ramaiah, G. K.: Analysis of vibration of clamped square plates by the Rayleigh-Ritz method with asymptotic solutions from a modified bolotin method. *Journal of Sound and Vibration*, 56, (1978), 127 – 135.

Wilson, J. F.; Henry, J. K.; Clark, R. L.: Measured free vibrations of partially clamped, square plates. *Journal of Sound and Vibration*, 231, (2000), 1311 – 1320.

Yang, X. L.; Sethna, P. R.: Local and global bifurcations in parametrically excited vibrations of nearly square plates. *Int. J. Non-Linear Mechanics*, 26, (1991), 199 – 220.

Yang, X. L.; Sethna, P. R.: Non-linear phenomena in forced vibrations of a nearly square plate: Antisymmetric case. *Journal of Sound and Vibration*, 155, (1992), 413 – 441.

Address:
Fabian Duvigneau
Institute of Mechanics, Otto-von-Guericke University, Universitätsplatz 2, D-39106 Magdeburg, Germany
Tel.: +49 391 67 52754
Fax: +49 391 67 12439
email: `fabian.duvigneau@ovgu.de`